BERKELEY LAB

CHARACTERIZING SNOWFALL AND SNOWPACK USING 60 GHZ MMWAVE RADAR SENSORS

Stijn Wielandt[1], Ivo Marković[1], Lonnie Chien[1], Diana Morales[1], Ryan Landon Crumley[2], Baptiste Dafflon[1], Reynold Cooper[3]
swielandt@lbl.gov

Lawrence Berkeley National Laboratory, Climate and Ecosystem Sciences Division (1) & Nuclear Science Division (3), 1 Cyclotron Rd, Berkeley, CA 94720, United States
Los Alamos National Laboratory, Climate, Ecosystems, and Environmental Science (2), Bikini Atoll Rd, Los Alamos, NM 87545, United States

U.S. DEPARTMENT OF ENERGY
Office of Science

INTRODUCTION

- Environmental scientists need spatiotemporally dense observations.
- Existing techniques for snowpack and snowfall monitoring are often inaccurate, low-resolution, high-power, labor-intensive, expensive.
- mmWave FMCW SoCs can be used to form networks of distributed radar sensors for high-resolution environmental observations

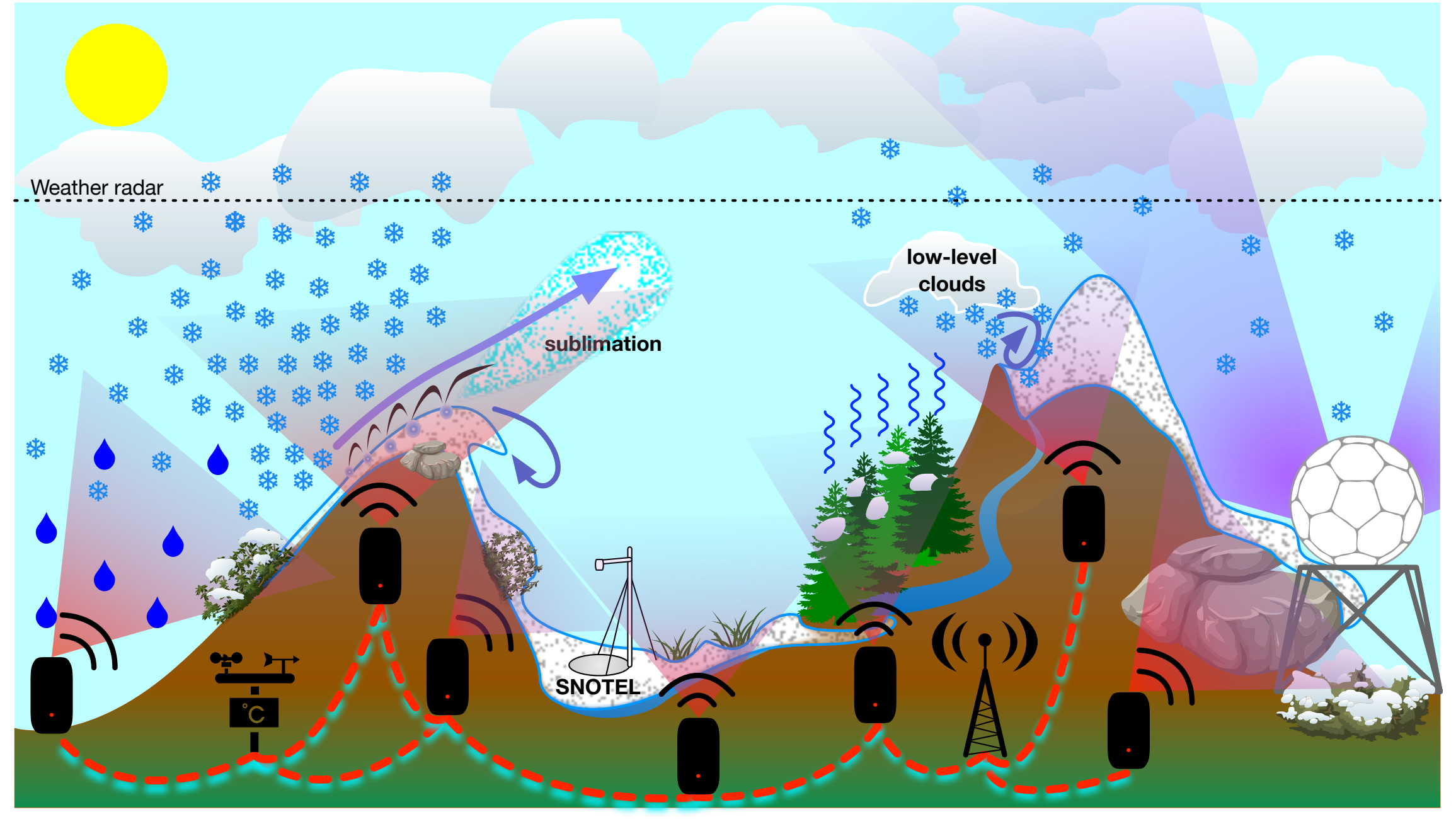

Fig. 1: Concept of distributed mmWave radars for monitoring environmental processes

ENVIRONMENTAL MMWAVE SENSORS

- We selected 60 GHz BGT60TR13C FMCW radar development kits for experiments in remote environments
- WiFi connectivity in remote field sites enables real-time UDP streams of raw ADC data and remote configuration by LBNL servers
- Low power consumption allows for operation on solar power

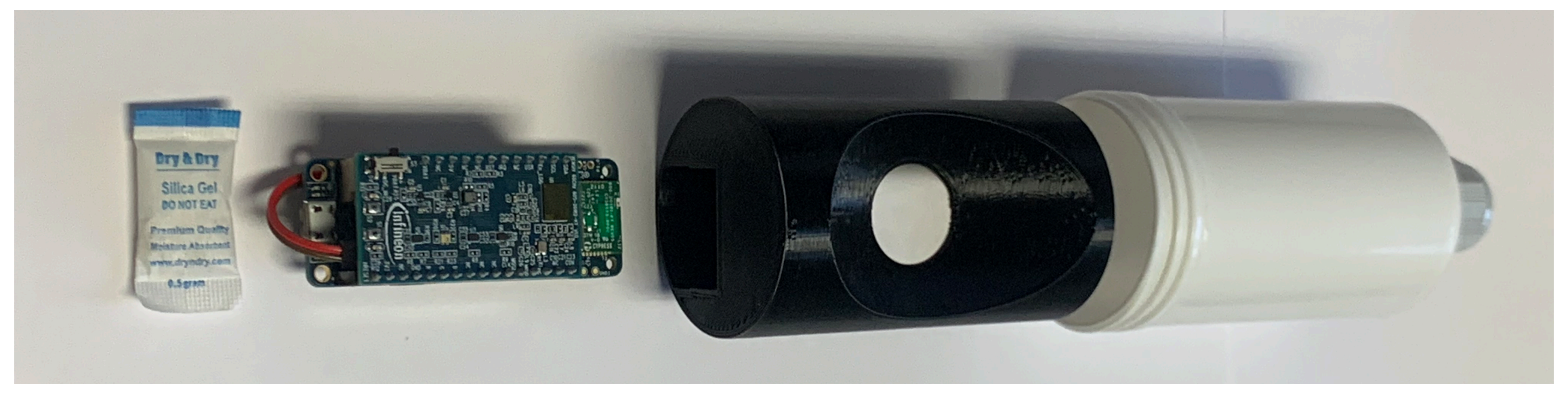

Fig. 2: Disassembled radar system for field deployment

- Compact 1Tx-3Rx on-chip antennas
- Enclosure/radome structure:
  - PP ($\varepsilon_r = 2.3, \tan\delta = 10^{-4}$)
  - Thickness = 1.65 mm = $\lambda/2$
  - Cylindrical with chip centered:
    - Far field (r = 24.5 mm)
    - Equidistance ensures constant radome thickness

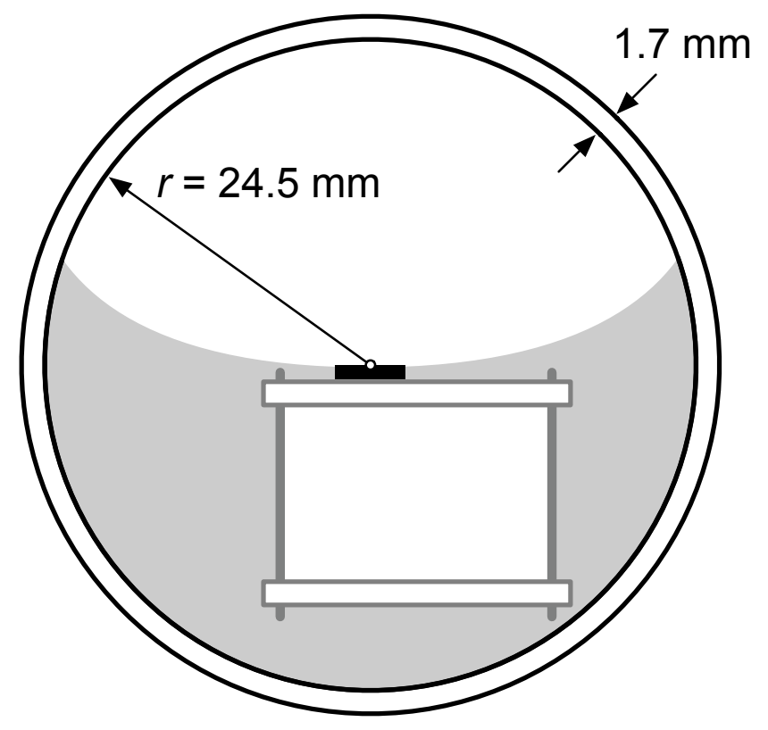

Fig. 3: Radome cross section

	A. SNOWPACK	B. SNOWFALL DOPPLER	C. SNOWFALL ATTENUATION
f_{start}	58.0 GHz	60.0 GHz	60.0 GHz
f_{stop}	63.5 GHz	60.2 GHz	60.4 GHz
Bandwidth	5.5 GHz	0.2 GHz	0.4 GHz
P_{Tx}	31dBm	31 dBm	31 dBm
$G_{RX,IF}$	38 dB	33 dB	45 dB
f_{sample}	2500 kHz	2500 kHz	2500 kHz
# Samples per chirp	512	64	512
# chirps/frame	256	128	16
Active Rx channels	[1, 2, 3]	[2]	[2]
Max. range	7 m	23.8 m	**97.3 m**
Range resolution	**0.028 m**	0.84 m	0.38 m
Range accuracy (air)	0.0137 m	0.372 m	0.19 m
Max. velocity	3.038 m/s	**15.4 m/s**	1.6 m/s
Velocity resolution	0.024 m/s	0.241 m/s	0.209 m/s
Velocity accuracy	0.012 m/s	0.120 m/s	0.104 m/s

Table 1: Radar configurations for the three studied scenarios

SNOWPACK PROFILING

- Snow height can be measured by performing downwards radar ranging from a pole to the top of the snowpack.
- Experiments performed in Nome, AK
- Range tests performed at (0.24, 0.39, 0.53, 0.63, 0.73, 1.31, 1.64) m
- A total of 3,200 radar frames were obtained over all 7 setups

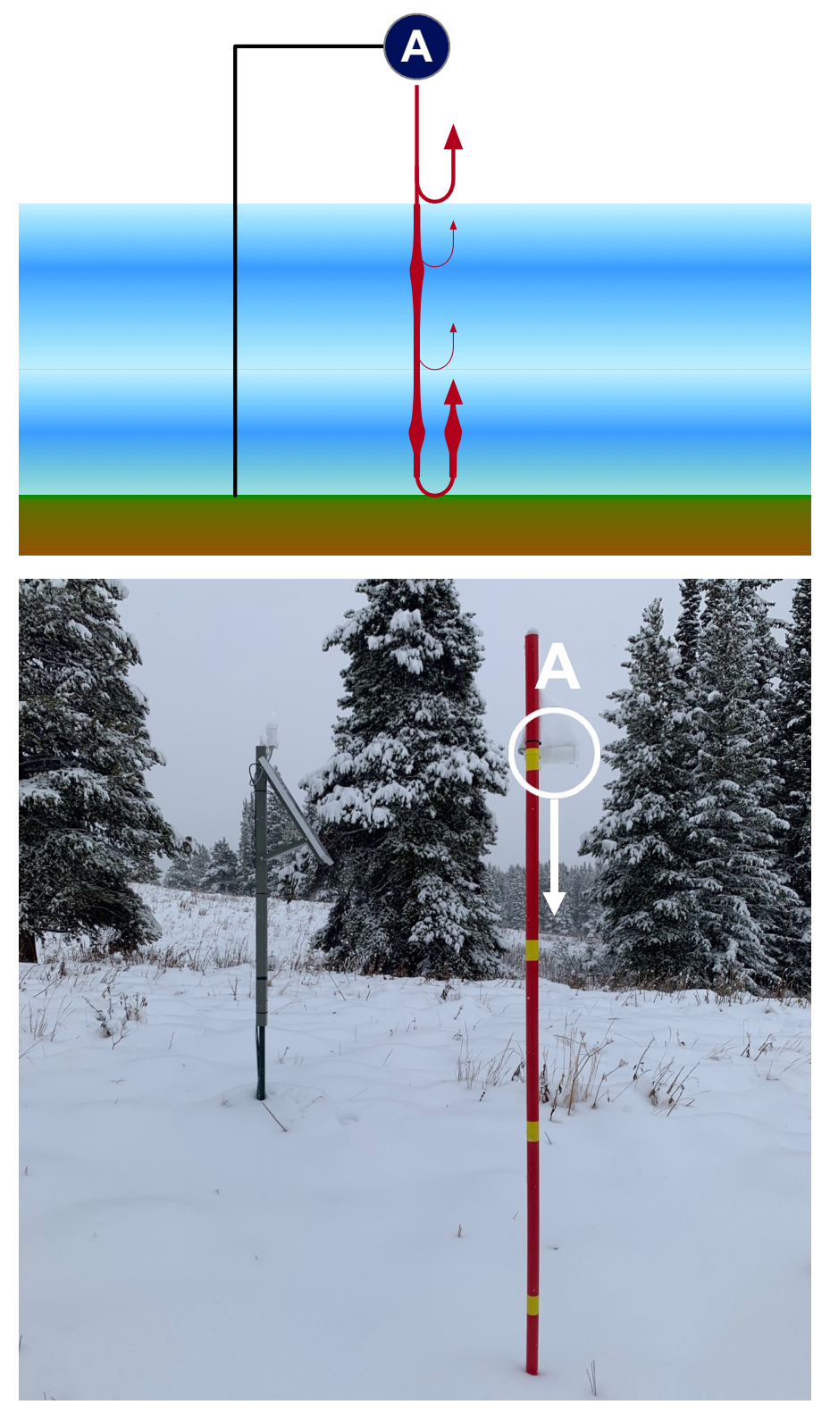

Fig. 4: Snowpack profiling setup

- We evaluate CA-CFAR for top-of-snowpack detection
  - Usually returns multiple peaks
  - Exact peak can be missed (Fig.5)
  - Not tailored to this problem
- We propose a novel algorithm:
  1) Steepest upslope in range plot: $x = \max(\nabla amplitude(range))$
  2) Detected top-of-snowpack $t(0)$ is first local maximum after slope $t = [amplitude'(range) \overset{?}{=} 0]\ \forall\ range > x$

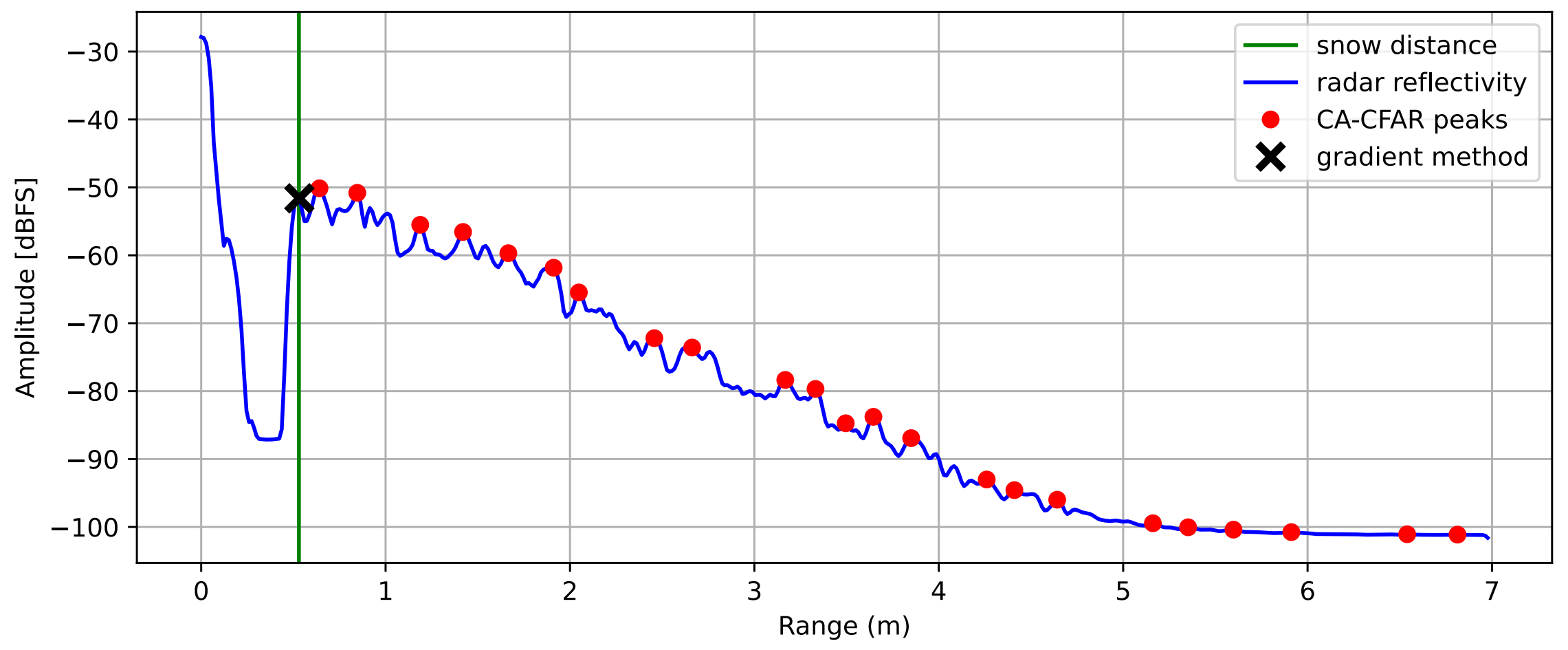

Fig. 5: Illustration of the proposed gradient based ranging algorithm compared to CA-CFAR

- CA-CFAR returns multiple peaks, so we evaluate two selection criteria (Max peak, First peak) and compare snow ranging errors to the proposed gradient based method.

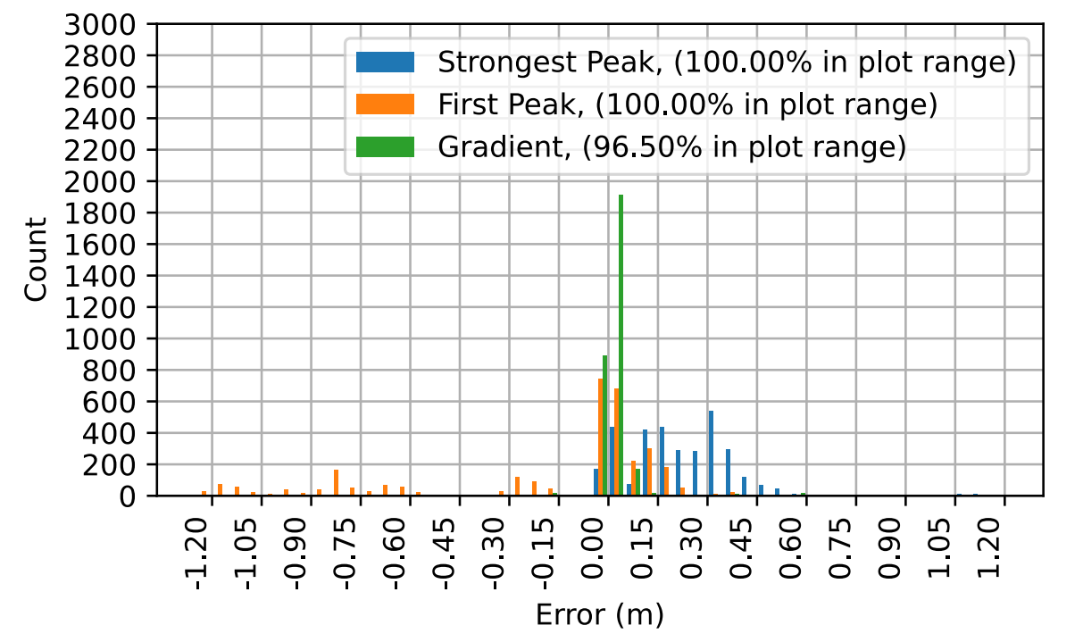

Error [m]	CA-CFAR Max peak	CA-CFAR First peak	Gradient
Mean	0.218	-0.179	0.076
Std.	0.160	0.395	0.314
P50	0.217	-0.006	0.002
P90	0.397	0.121	0.053
P95	0.443	0.183	0.454

Fig. 6: Snow height estimation errors for the gradient based algorithm and CA-CFAR

- The gradient based method provides most accurate results with significant outliers. We evaluate range profile averaging methods:
  - Averaging channels drastically reduces errors
  - Antennas perform equally
  - Range profile averaging over multiple radar frames drastically reduces outliers

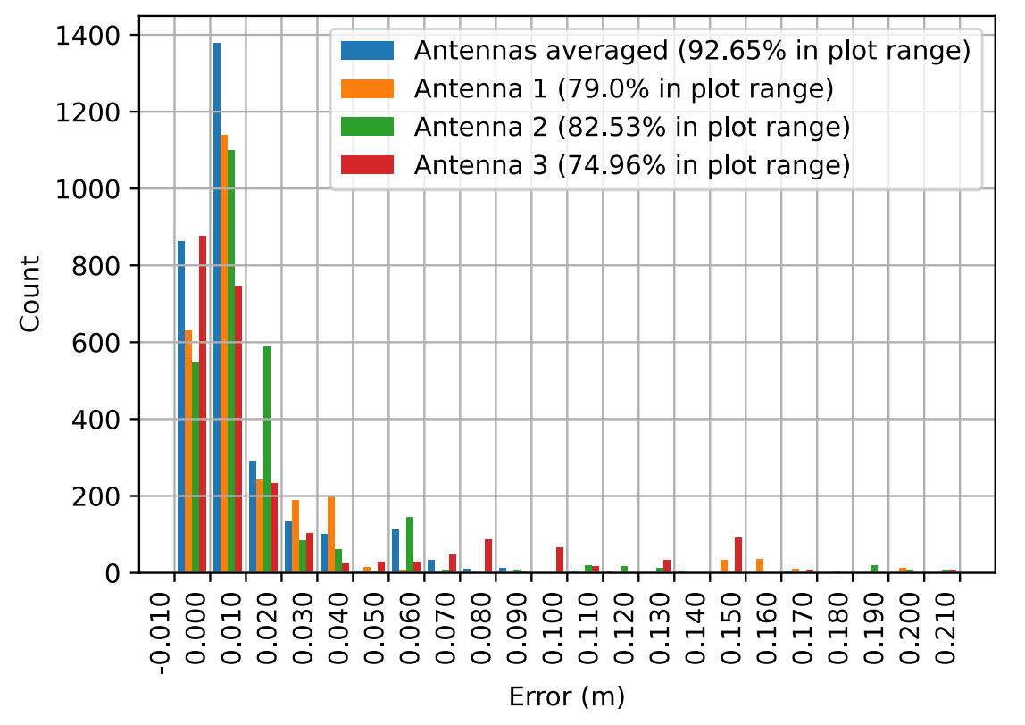

Error [m]	Ant. 1	Ant. 2	Ant. 3	Ant. Avg.
Mean	0.189	0.176	0.134	0.076
Std.	0.415	0.442	0.434	0.314
P50	0.006	0.007	0.001	0.002
P90	0.943	0.698	0.238	0.053
P95	1.241	1.412	1.241	0.454

Fig. 7: Gradient based ranging errors for three Rx channels and their averaged range profiles

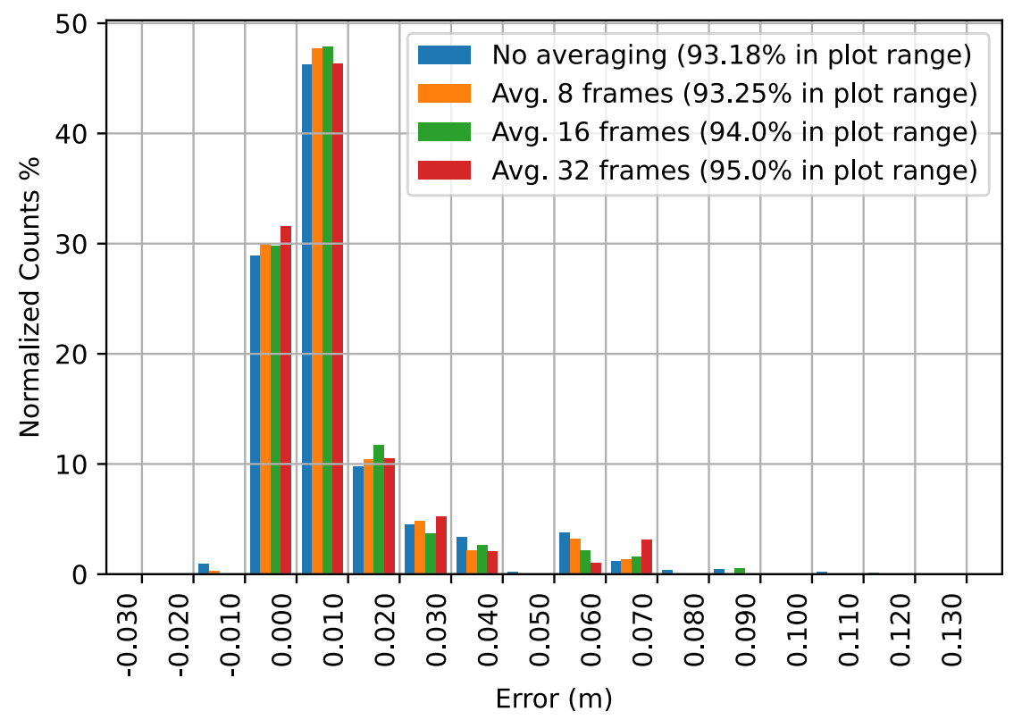

Error [m]	1 Frame	8 Avg.	16 Avg.	32 Avg.
Mean	0.076	0.027	0.024	0.019
Std.	0.314	0.169	0.155	0.128
P50	0.002	0.002	0.002	0.002
P90	0.053	0.025	0.025	0.025
P95	0.454	0.053	0.053	0.042

Fig. 8: Gradient based ranging errors for averaged range profiles over multiple frames

Snow-water equivalent (SWE) and snowpack morphology:

- Snowpack permittivity affects radar signal propagation speed
  - $\varepsilon_{r,\text{dry snow}}$ only depends on density (ρ [kg/m^3]), not morphology
  - $\varepsilon_{r,\text{dry snow}} = 1 + 1.7\rho + 0.7\rho^2$ (Tiuri et al. 1984)
  - Snowpack analysis enables range profile correction (Fig. 9)
  - Inversely: range-to-ground knowledge enables snow density and SWE measurement
  - Morphology affects reflectivity so range profiles indicate layers

M. Tiuri, A. Sihvola, E. Nyfors and M. Hallikaiken, "The complex dielectric constant of snow at microwave frequencies," in *IEEE Journal of Oceanic Engineering*, vol. 9, no. 5, pp. 377-382, December 1984, doi: 10.1109/JOE.1984.1145645.

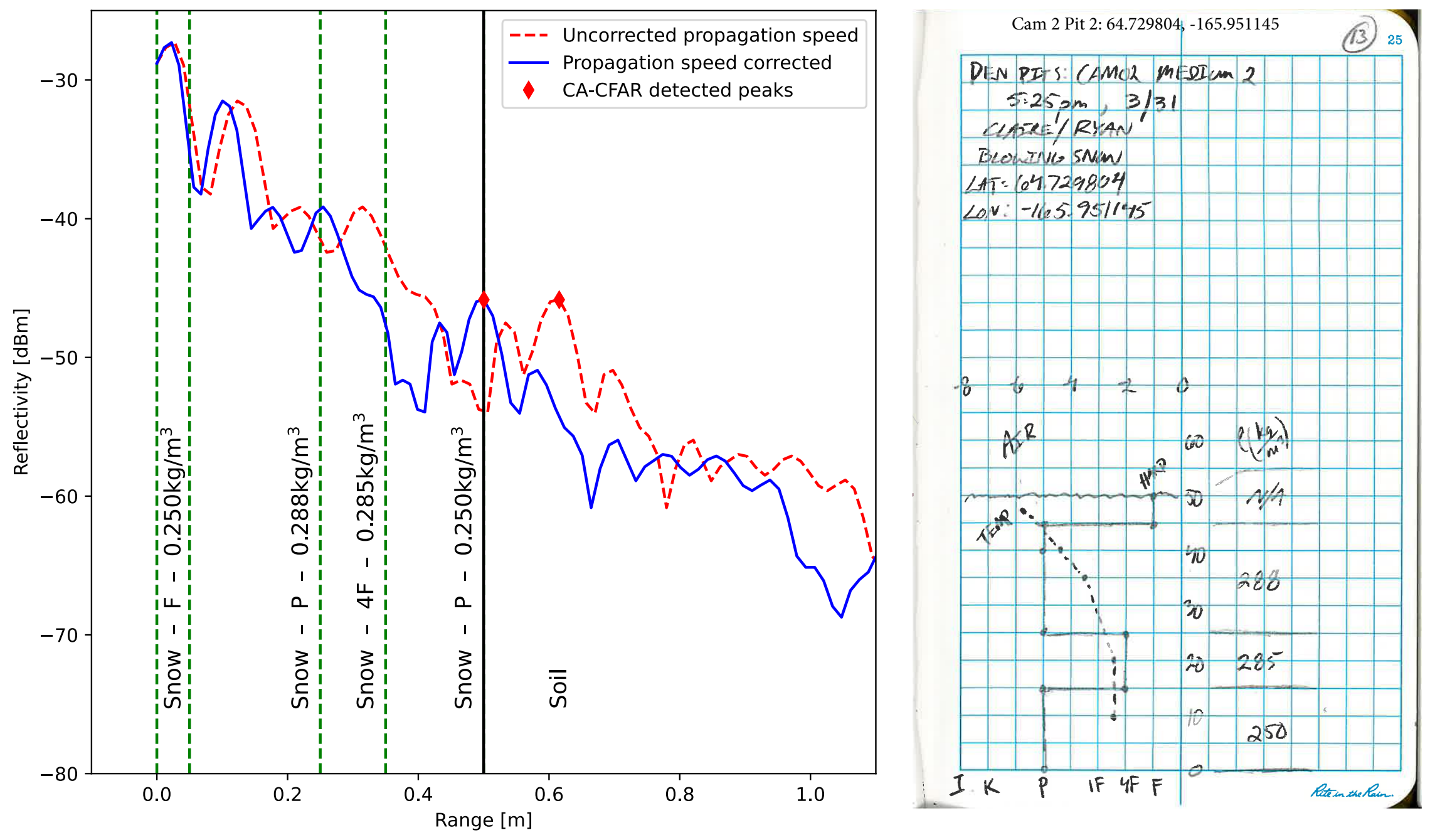

Fig. 9: Snow density corrected range plot (left) and conventional snowpack analysis (right)

SNOWFALL CHARACTERIZATION

mmWave as small-scale, high-resolution weather radars:

B. Upwards pointing radars to measure velocity and reflectivity of hydrometeors

C. Horizontally pointing radars to measure wind direction and speed. In combination with radar targets, attenuation measurements can provide more accurate information on precipitation intensity

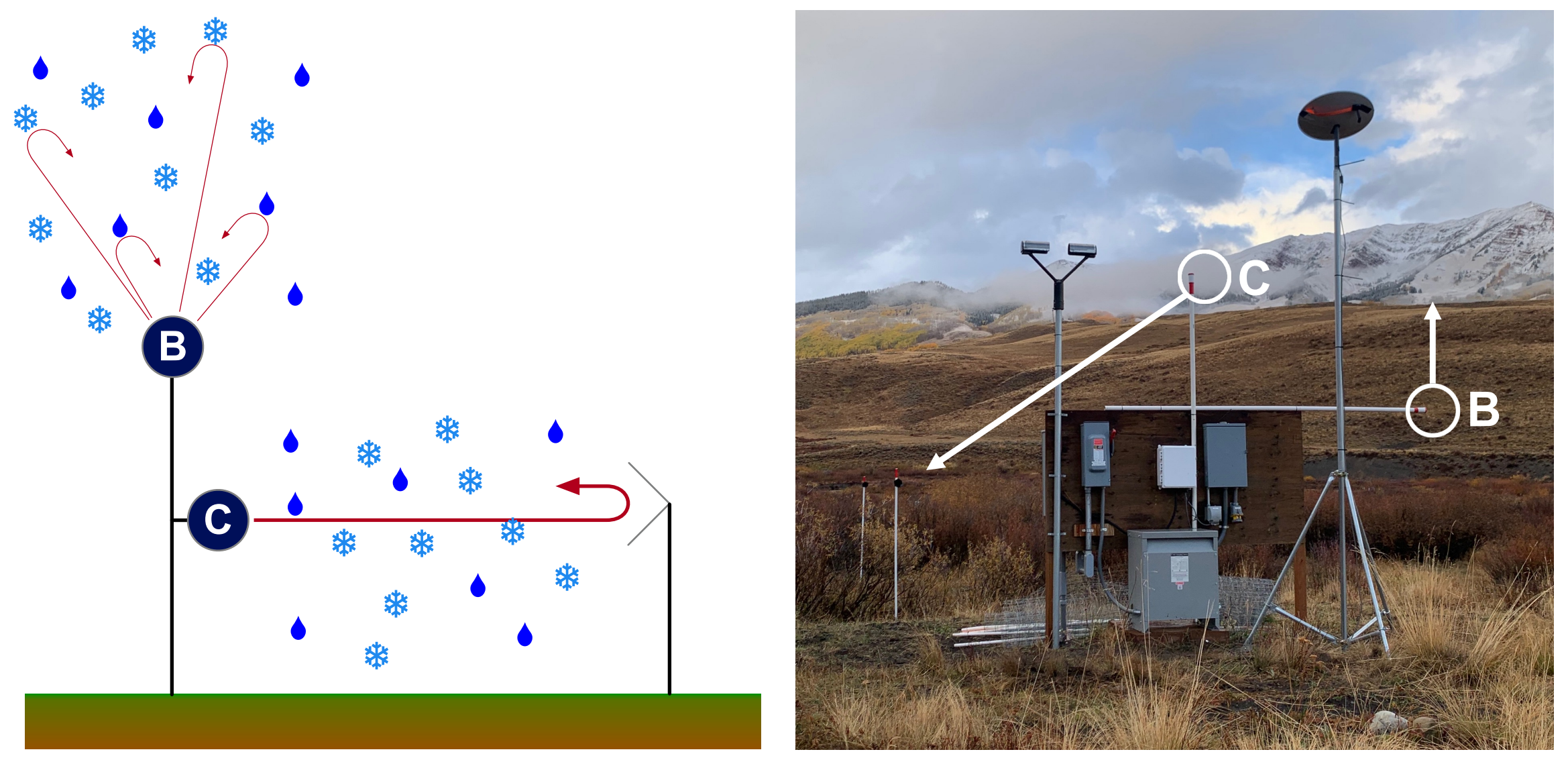

Fig. 10: Snowfall characterization setup based on doppler velocity (B) or signal attenuation (C)

B. Doppler based precipitation characterization

- Rain observability is high due to strong reflectivity ($\varepsilon_{r,\text{water}} = 12$) and high velocity
- (Dry) snow observability is lower due to low reflectivity ($\varepsilon_{r,\text{dry snow}} \approx 2$) and low velocity

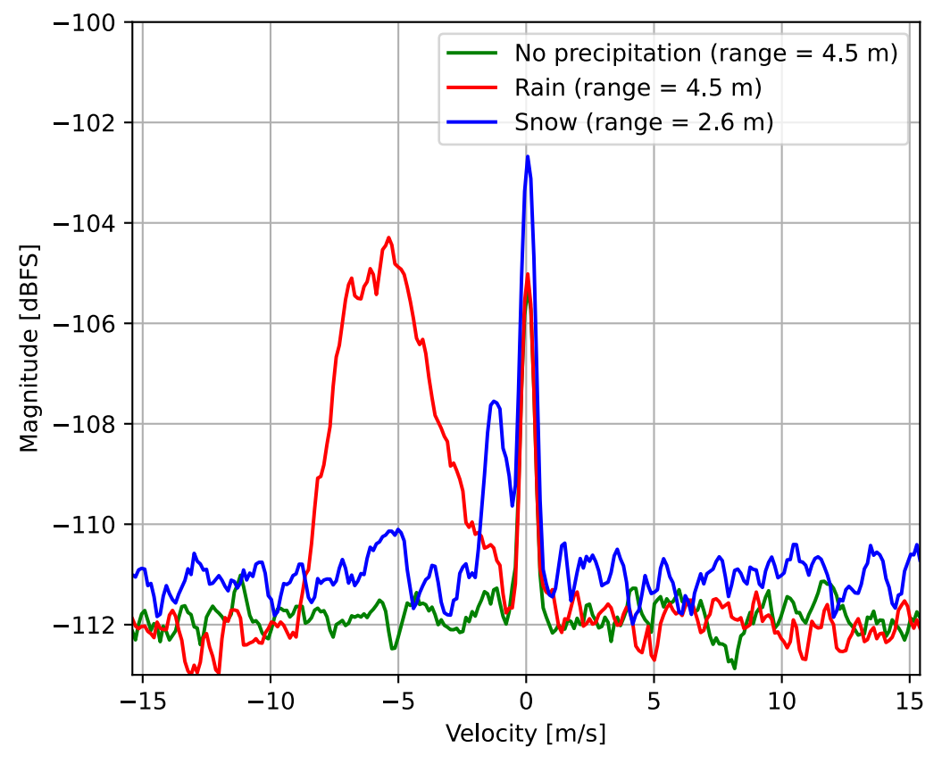

Fig. 11: Velocity profile with precipitation events

- Dry weather observations show only zero-doppler reflections (avg. 351 frames over 70 seconds interval)
- Ground truth data obtained with co-located laser curtain based disdrometer, measuring hydrometeor speed, size, type, etc.

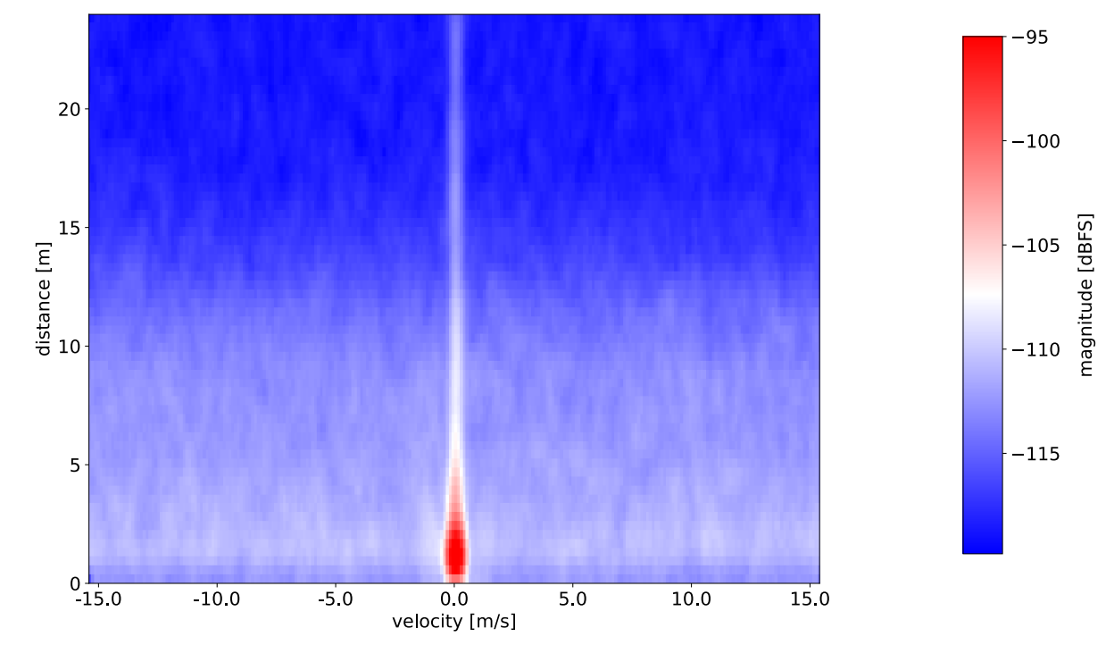

Fig. 12: Range-velocity plot for dry weather

- Rain observations match disdrometer velocity measurements. Radar reflectivity aligns with water volume corrected particle counts (avg. 180 frames over 70 seconds interval)

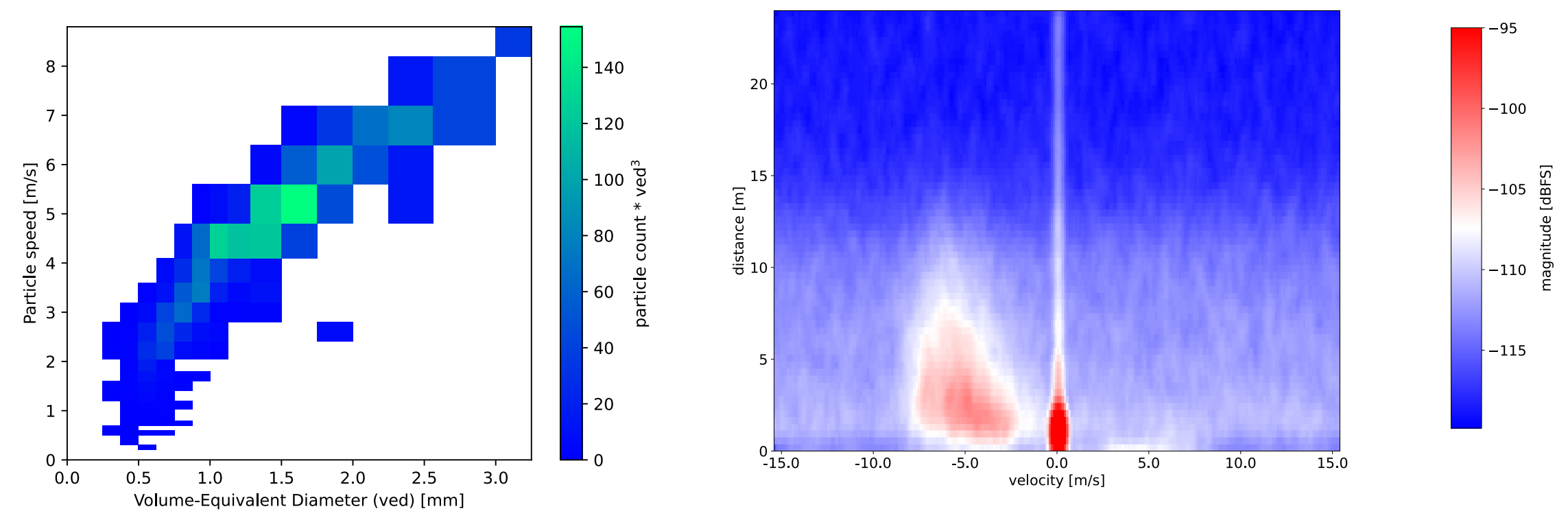

Fig. 13: Disdrometer rain particle measurement (Left), and radar range-velocity plot (Right)

- Snow observations match disdrometer velocity measurements. Radar reflectivity aligns with disdrometer particle counts (avg. 306 frames over 70 seconds interval)

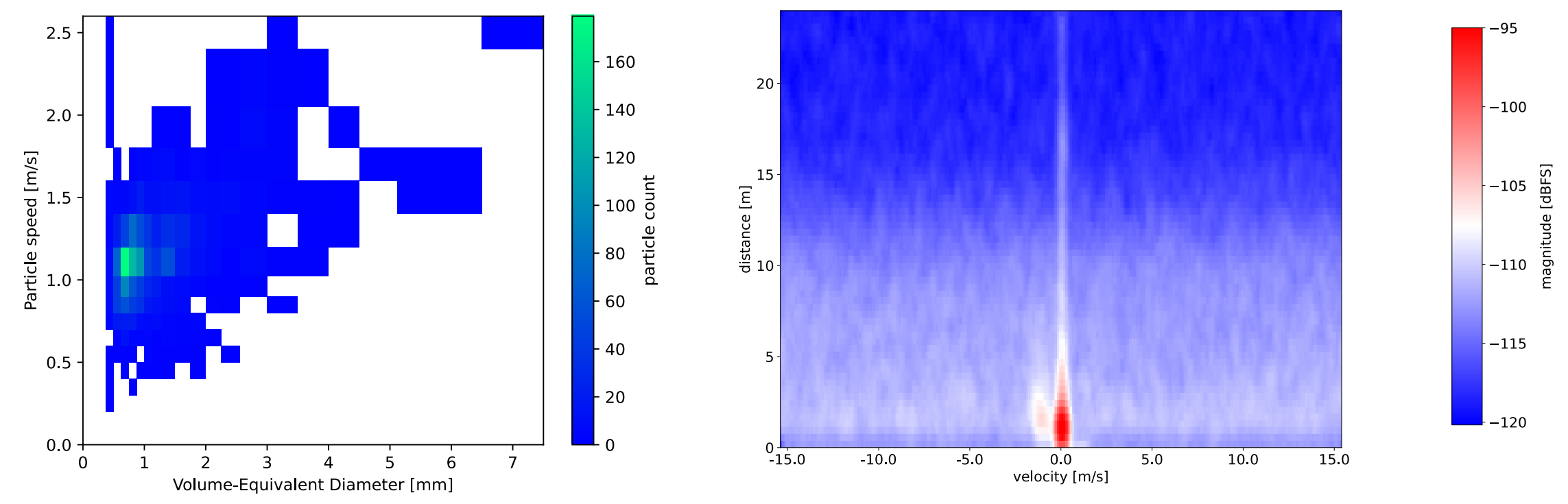

Fig. 14: Disdrometer snow particle measurement (Left), and radar range-velocity plot (Right)

C. Attenuation based precipitation characterization using radar targets

- Two-way signal attenuation due to hydrometeors is proportional to radar target distance and precipitation intensity

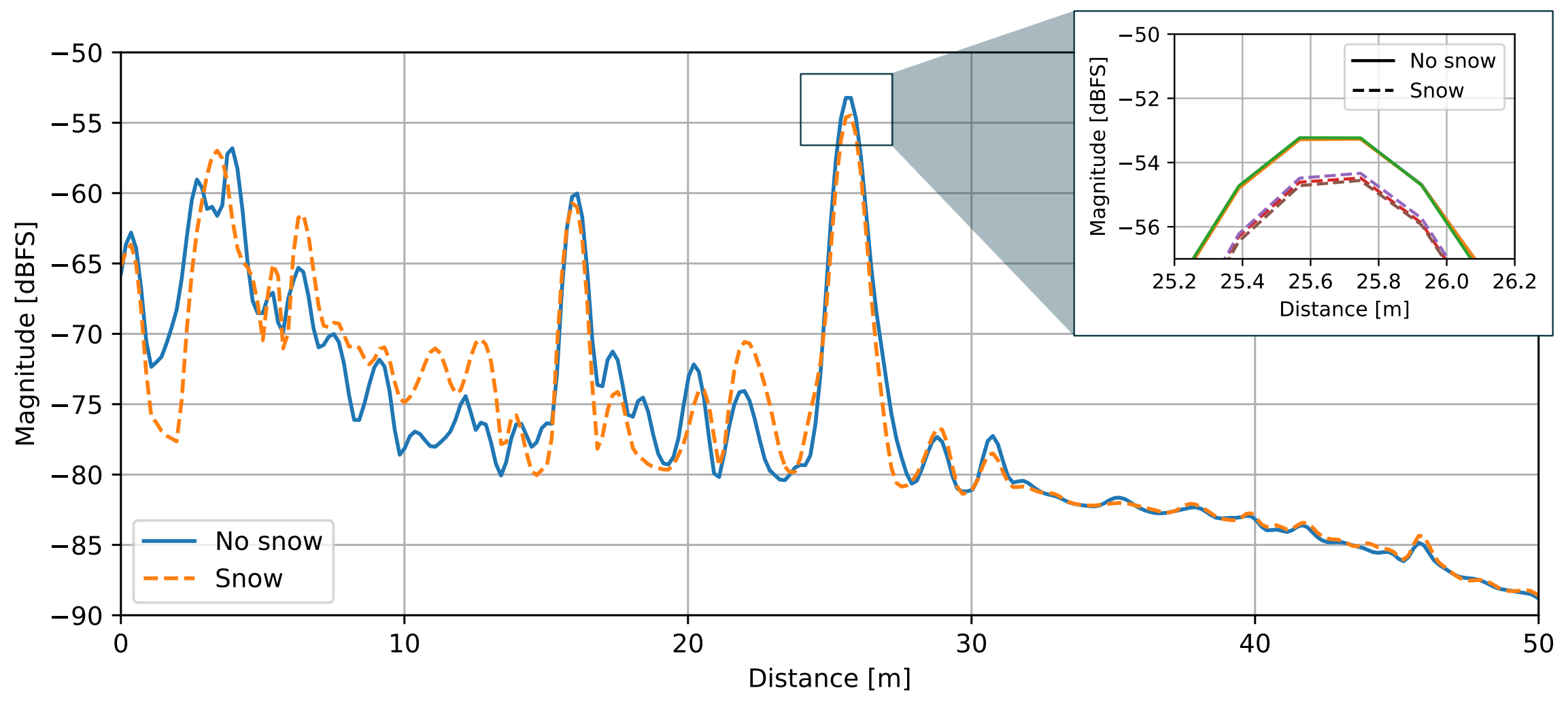

Fig. 15: Snow induced attenuation of a radar signal that is reflected off a distant target

CONCLUSIONS AND FUTURE WORK

- Low-cost 60 GHz radar SoCs can be used for high-resolution, real-time snow observations. The compactness and low power consumption of the system enables remote deployments
- A gradient based algorithm combined with averaging over frames and Rx channels enables snow height detection with cm-precision
- Range-to-ground knowledge enables a precise calculation of snow density through signal propagation speed corrections
- Upwards pointing radars accurately measure hydrometeor speed
- Horizontally pointing radars capture atmospheric attenuation that is proportional to distance and precipitation intensity

Future work:

- Use ML to detect the structure and density of snowpack layers
- Quantify precipitation based on attenuation measurements, measure wind speed, and classify precipitation using ML

ACKNOWLEDGEMENT

This work was supported by the U.S. Department of Energy, Office of Science, Office of Biological and Environmental Research, Next-Generation Ecosystem Experiments–Arctic Project (NGEE-Arctic), the LBNL Watershed Function Scientific Focus Area (WF-SFA), and the Laboratory Directed Research and Development Program of Lawrence Berkeley National Laboratory under U.S. Department of Energy Contract No. DE-AC02-05CH11231.